X-Ray Investigations on Molten Cu–Sb Alloys

Th. Halm, H. Neumann, and W. Hoyer

Technische Universität Chemnitz–Zwickau, PSF 964, 09009 Chemnitz, Germany

Z. Naturforsch. **49a**, 530–534 (1994); received February 28, 1994

Using X-ray diffraction, structure factors and pair correlation functions of several molten Cu–Sb alloys and pure antimony were determined and compared with published structural, thermodynamic and electronic properties. The eutectic concentration $Cu_{37}Sb_{63}$ was investigated in dependence on temperature, and a model structure factor was calculated applying a segregation model.

Experimentals

The scattering intensities were measured with a $\Theta-\Theta$ diffractometer (Mo–Kα) described in [1].

After corrections for polarization [2] and normalization, the Compton-scattering [3] was subtracted and the structure factor in the Faber-Ziman-Form [4] was calculated, using the equation

$$S(Q) = \frac{I_A^{\text{coh}} - \langle f^2 \rangle + \langle f \rangle^2}{\langle f \rangle^2}, \quad (1)$$

$$\langle f^2 \rangle = c_1 f_1^2 + c_2 f_2^2,$$

$$\langle f \rangle^2 = (c_1 f_1 + c_2 f_2)^2.$$

Here, $Q = (4\pi/\lambda)/\sin\theta$ denotes the magnitude of the momentum transfer and I_A^{coh} the coherent scattering intensity per atom, while f_i refers to the atomic scattering factor [5] corrected for anomalous dispersion [6], and c_i to the fraction of the atoms i, respectively.

The pair correlation function was calculated by the equation

$$g(r) = 1 + \frac{1}{2\pi^2 r \varrho_0} \int_0^{Q_{\text{Max}}} Q\,[S(Q)-1]\sin Qr\,\mathrm{d}Q, \quad (2)$$

where ϱ_0 is the average number density, and Q_{Max} the maximum momentum transfer reached in the scattering experiment. $S(Q)$ was extrapolated to an approximate value of $S(0)$ [7] to minimize truncation errors by the lower integration limit.

Results

The obtained structure factors are shown in Figure 1. With increasing concentration of antimony the "shoulder" at the low Q-side of the structure factor's main peak grows, while the height of the main peak decreases. The higher oscillations of the structure factors become weaker. The shoulder appears at a position where the structure factor of antimony possesses its main peak.

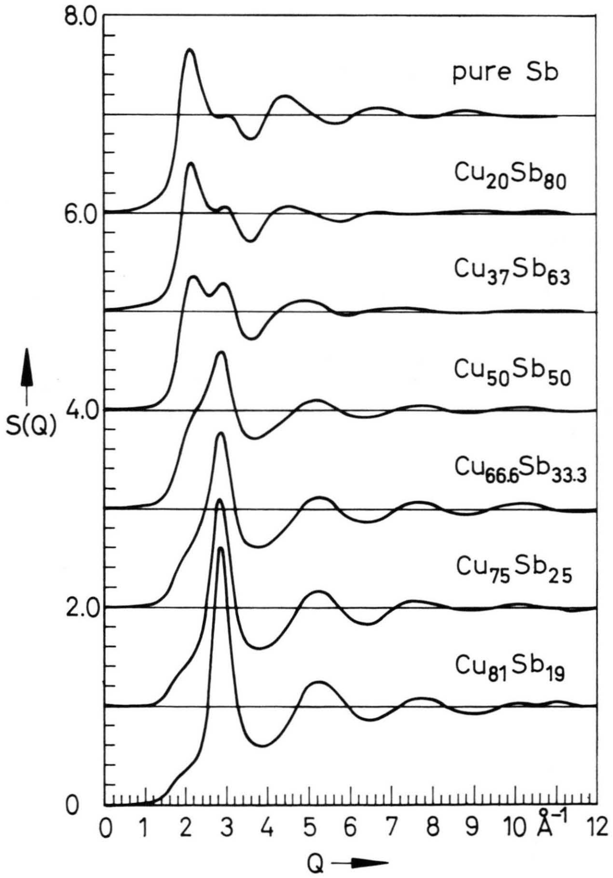

Fig. 1. Structure factors of molten Cu–Sb alloys.

Reprint requests to Prof. Dr. W. Hoyer, Technische Universität Chemnitz–Zwickau, PSF 964, 09009 Chemnitz.

0932-0784 / 94 / 0400-0530 $ 01.30/0. – Please order a reprint rather than making your own copy.

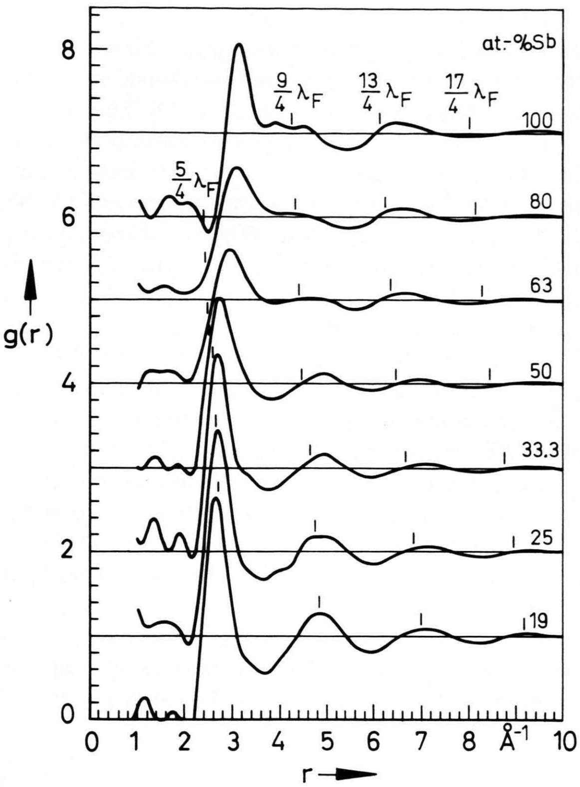

Fig. 2. Pair correlation functions of molten Cu–Sb alloys. The bars indicate the minima of the Friedel-oscillations (see text).

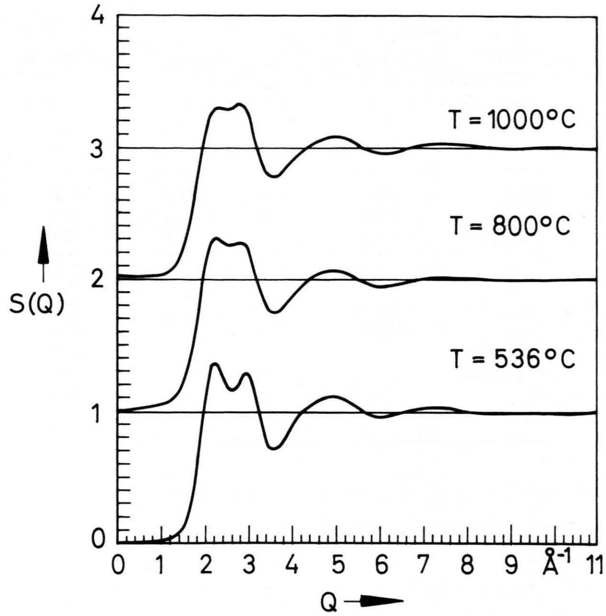

Fig. 3. Structure factors of the molten eutectic $Cu_{37}Sb_{63}$ at different temperatures.

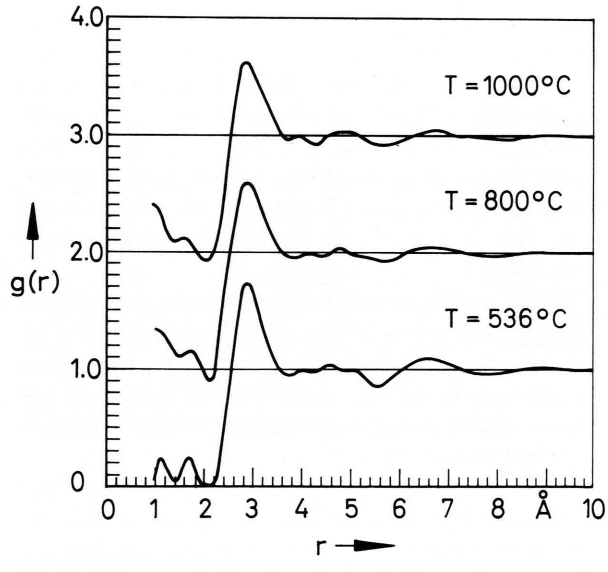

Fig. 4. Pair correlation functions of the molten eutectic $Cu_{37}Sb_{63}$ at different temperatures.

At the eutectic concentration $Cu_{37}Sb_{63}$ a splitting of the main peak is found.

The structure factor of $Cu_{20}Sb_{80}$ shows a similar shape as that of pure molten antimony because of the dominating weighting factor of the Sb–Sb correlation in this alloy.

The pair correlation functions (Fig. 2) of the copper-rich samples possess a relatively high and symmetrical main peak, the further oscillations are well-pronounced. With increasing antimony content the height of the main peak of $g(r)$ decreases and it becomes broader. The second peak becomes weaker and almost vanishes in the case of the samples $Cu_{37}Sb_{63}$ and $Cu_{20}Sb_{80}$.

The eutectic $Cu_{37}Sb_{63}$ was investigated at different temperatures (Figure 3). The structure factor shows a temperature-dependent change of the main peak in such a way, that the splitting is less-pronounced if the temperature increases. It is worthwile noting that the first hump of the main peak decreases, while the second remains almost unchanged. In the pair correlation functions (Fig. 4) the temperature-dependent changes are weak, the main peak becomes slightly broader with increasing temperature.

Table 1 contains the distance r^{I} of nearest neighbours and the coordination number of the first shell.

Table 1. X-ray weighted distance of nearest neighbours r^{I} and coordination number of the first shell (N_{Min} and N_{Sym} are obtained from integration up to the first minimum and from the first shell assumed to be symmetrical).

Alloy	Temp. °C	r^{I} Å	N_{Sym}	N_{Min}
$Cu_{81}Sb_{19}$	650	2.64	8.2	11.2
$Cu_{75}Sb_{25}$	690	2.68	7.8	9.9
$Cu_{66.6}Sb_{33.3}$	690	2.67	5.5	8.3
$Cu_{50}Sb_{50}$	750	2.70	5.0	7.8
$Cu_{37}Sb_{63}$	536	2.91	7.0	6.7
$Cu_{37}Sb_{63}$	800	2.86	7.0	6.6
$Cu_{37}Sb_{63}$	1000	2.84	7.0	6.9
model (Cu_2Sb)		2.93	7.7	6.9
model (Cu_3Sb)		2.94	7.8	6.9
$Cu_{20}Sb_{80}$	540	3.06	6.6	6.0
pure Sb	654	3.08	5.1	5.2

With increasing concentration of antimony r^{I} also increases, while the coordination number becomes smaller.

In the case of $Cu_{37}Sb_{63}$ r^{I} slightly decreases if the temperature is increased.

Discussion

A comparison with the results of Knoll and Steeb [8], who described X-ray and neutron scattering investigations on molten alloys of the same system, shows a principle qualitative agreement but differences in the quantitative behaviour. A splitting of the structure factor's main peak into two nearly equally high subpeaks does not appear in [8] until $Cu_{20}Sb_{80}$ (in our case this is already to be found at the eutectic $Cu_{37}Sb_{63}$).

In the concentration range of 15 to 61 at.-% Sb the existence of clusters having a composition like Cu_2Sb was stated in [8]. Measurements of the resistivity lead to a maximum at 25 at.-% Sb followed by a broad but flat minimum centered around the eutectic composition (Steeb et al. [9]).

Viscosity measurements done by Bienias and Sauerwald [10] show an inflection point at 35 at.-% Sb; with decreasing temperature the viscosity increases rapidly in the concentration range below 35 at.-% Sb. Furthermore, the measured values are larger than expected for a statistical distribution.

Takeuchi et al. [11] reported that the heat of mixing of liquid Cu–Sb alloys possesses a dip at about 24 at.-% Sb, which is in accordance with the minimum found in the curve given by Hayer et al. [12]. The authors of [12] also found peaks in the excess heat capacity at 25 and 50 at.-% Sb.

In the thermopower, experimentally determined by Matsuura et al. [13], a decrease up to a Sb-concentration of about 15 at.-%, followed by a broad peak centered at 50 at.-% Sb is to be seen. All these results indicate a tendency of compound formation in the liquid state. The clusters are assumed to have a composition similar to the compounds Cu_2Sb and Cu_3Sb existing in the solid phase. Whether these clusters, built up in the melt, are only of one type of composition or if clusters with different compositions occur, can not be clearly answered.

A characteristic feature of the alloys from the system Cu–Sb is a peak in the structure factors at about 3 $Å^{-1}$, it occurs as a shoulder for antimony-rich alloys and is the main peak for copper-rich alloys.

According to Hafner [14] this peak can be understood as electronically-induced, indicating the influence of the electron system on the structure. The peak should appear at a position close to $2k_{\mathrm{F}}$, where k_{F} is the Fermi-wavevector.

It was shown for various binary "nobel metal–polyvalent element" alloys that the position Q_{Pe} of this subpeak shifted towards $2k_{\mathrm{F}}$ if the mean number of valence electrons per atom

$$\bar{Z} = c_1 Z_1 + c_2 Z_2 \tag{3}$$

comes closer to a value of 1.8 and, consequently, for $z = 1.8$ one obtains $Q_{\mathrm{Pe}} = 2k_{\mathrm{F}}$ (Häussler [15]). In (3), Z_i and c_i are the number of valence electrons and the concentration of the component i, respectively.

The Friedel-wavelength λ_{F}, due to the oscillations of the effective pair potential of the ion-ion interaction, is connected to $2k_{\mathrm{F}}$ according to

$$\lambda_{\mathrm{F}} = \frac{2\pi}{2k_{\mathrm{F}}}. \tag{4}$$

If the peaks of the pair correlation function are observed at positions

$$r = (n + \tfrac{1}{4})\,\lambda_{\mathrm{F}}, \qquad n = 1, 2, 3, \ldots \tag{5}$$

the ions sit in the minima of Friedel-oscillations, which is a favourable structural arrangement.

The values of k_{F} for the different alloys were calculated in the free electron approximation by

$$k_{\mathrm{F}} = \sqrt[3]{3\pi^2 \varrho_0 \bar{Z}}. \tag{6}$$

Figure 5 shows a plot of the calculated values of $2k_{\mathrm{F}}$ against the experimental values of Q_{Pe}. The curves cross at a concentration near 20 at.-% Sb (which cor-

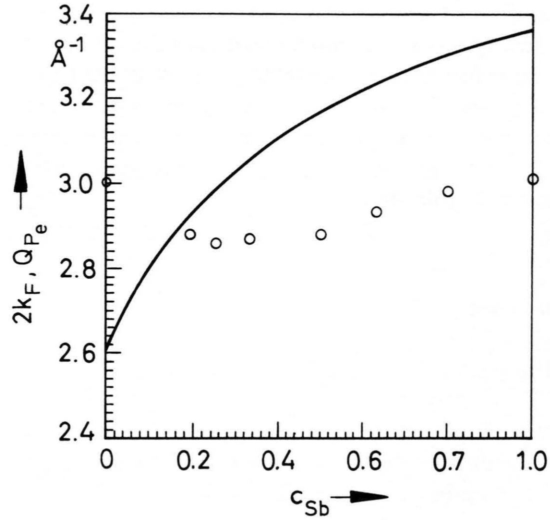

Fig. 5. Experimental peak positions Q_{P_e} and calculated values of $2k_F$ (full line). (The experimental value for Cu was taken from Waseda [17].)

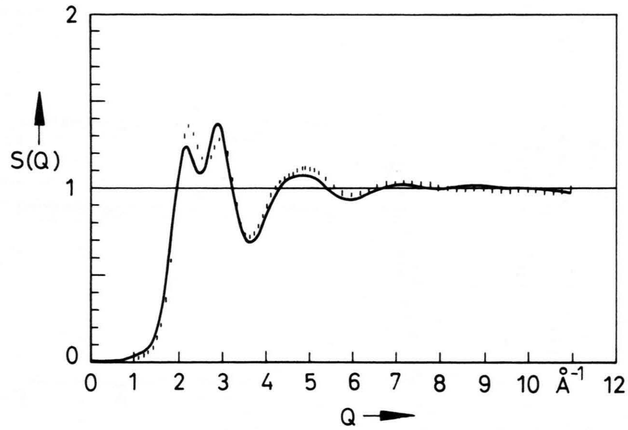

Fig. 7. Structure factor of the molten eutectic $Cu_{37}Sb_{63}$, calculated by the segregation model (line) assuming Cu_3Sb clusters, and experimental values at 536 °C (presented by error bars)

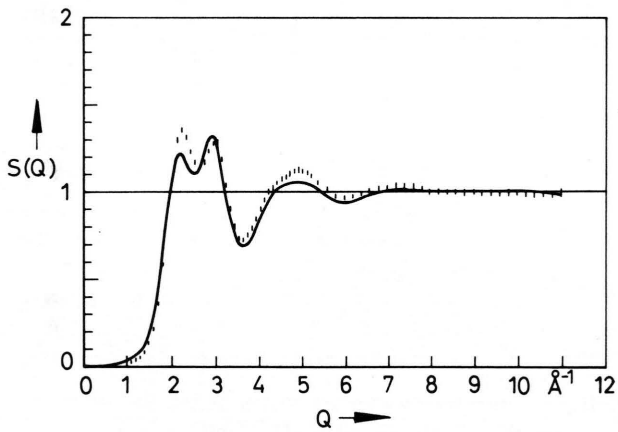

Fig. 6. Structure factor of the molten eutectic $Cu_{37}Sb_{63}$, calculated by the segregation model (line) assuming Cu_2Sb clusters, and experimental values at 536 °C (presented by error bars).

responds to 1.8 valence electrons per atom) as predicted by Häussler.

As seen from Fig. 2, the peaks in $g(r)$ of the copper-rich alloys Cu_2Sb, Cu_3Sb, and $Cu_{81}Sb_{19}$ are nearly at positions which correspond to the minima of the Friedel-oscillations.

If the content of Sb in the alloys is increased, the peak-positions in $g(r)$ deviate more and more from the positions of the minima due to the Friedel-oscillations.

For the alloys containing more than 61 at.-% Sb, a segregation tendency was suggested by Knoll and Steeb [8] which conforms with the slightly positive enthalpy of formation [12] as well as the maximum in the thermopower not far from the eutectic composition [13].

Therefore, we calculated the structure factor of $Cu_{37}Sb_{63}$ using a segregation model suggested in [16]. This model assumes segregation of the eutectic melt into clusters having a structure like the eutectic constituents. The clusters themselve are assumed to have a size such that only the coherent scattering due to correlations of atoms within the clusters significantly contributes to the whole coherent scattering of the melt. Then, the whole coherent scattering may be expressed as the sum of the coherent scattering intensities due to each type of cluster, weighted by the sum of the concentration of each atom type in each cluster:

$$I_{\text{coh}} = (c_1^1 + c_2^1)\, I_{\text{coh}}^1 + (c_1^2 + c_2^2)\, I_{\text{coh}}^2 . \tag{7}$$

c_j^i – concentration of atom type j in cluster type i.

For the eutectic melt $Cu_{37}Sb_{63}$, segregation into clusters corresponding to the eutectic constituents Cu_2Sb and Sb is assumed. The clusters should have a structure like that in the molten compound Cu_2Sb and molten Sb. A second run was done, assuming clusters of type Cu_3Sb instead of Cu_2Sb.

For both, molten Cu_2Sb (or Cu_3Sb, respectively) and Sb, the coherent scattering intensity was obtained

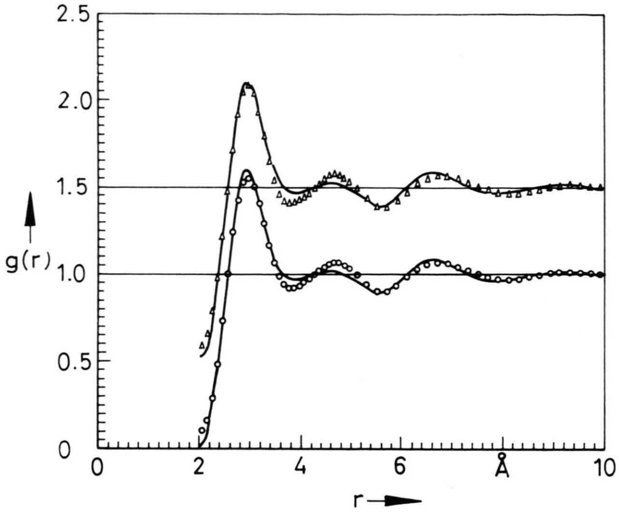

Fig. 8. Pair correlation function of the model structure factor and the experimental one at 536 °C: *line*: experimental, *circles*: assuming clusters of Cu_2Sb, *triangles*: assuming clusters of Cu_3Sb. (In the Fourier-transformation a damping function was used to reduce termination ripples in the second maximum.)

by single experiments earlier, and the model structure factors calculated from the intensities yielded by (7) are shown in Figs. 6 and 7.

It was found that the calculated structure factor in general agrees with the experimental one for both assumptions, clusters of Cu_2Sb and Cu_3Sb. Only in the low Q-region the model structure factor exceeds the error bars due to the statistical error of the experimental one. A good agreement between model and experiment can also be established for the pair correlation functions (Fig. 8), distances r^1 and coordination numbers (Table 1).

Conclusion

The peak in the structure factors located at about 3 $Å^{-1}$ is interpreted as a sign of the electronic influence on the structure. For the copper-rich alloys, good agreement between the position of the maxima in $g(r)$ and the minima in the Friedel-oscillations was found, indicating an electronically stabilized structure. For the alloy with 19 at.-% copper, the position of the structure factor's main peak is practically $2k_F$.

For the eutectic $Cu_{37}Sb_{63}$, segregation into clusters corresponding to an association of Sb-atoms and an association of unlike atoms is stated and examined by a segregation model suggested in [16], for which good agreement was found.

[1] W. Hoyer, E. Thomas, and M. Wobst, Kristall und Technik **15,** 903, (1980).
[2] K. Sagel, Tabellen zur Röntgenstrukturanalyse, Springer-Verlag, Berlin 1958.
[3] G. Palinkas, Acta Cryst. **A 29,** 10 (1973).
[4] T. E. Faber and J. M. Ziman, Phil. Mag. **11,** 153 (1965).
[5] P. A. Doyle and P. S. Turner, Acta Cryst. **A 24,** 390 (1968).
[6] D. T. Cromer and D. Liberman, Los Alamos Scientific Laboratory, University of California Report, LA-4403, UC-34, 1970.
[7] H. Neumann, W. Matz, and W. Hoyer, Exp. Technik Phys. **36,** 105 (1988).
[8] W. Knoll and S. Steeb, Phys. Chem. Liquids **4,** 39 (1973).
[9] S. Steeb, U. Maier, and D. Godel, Phys. Chem. Liquids **1,** 221 (1969).
[10] A. Bienias and F. Sauerwald, Z. anorg. allg. Chem. **161,** 51 (1927).
[11] S. Takeuchi, O. Uemura, and S. Ikeda, Sci. Rep. Res. Insts. Tohoku Univ. **A 25** (1974) No. 2–3, 41.
[12] E. Hayer, K. L. Komarek, and R. Castanet, Z. Metallk. **68,** 688 (1977).
[13] M. Matsuura and K. Suzuki, Phil. Mag. **31,** 969 (1975).
[14] J. Hafner, From Hamiltonians to Phase Diagrams, Springer Verlag, Berlin 1987.
[15] P. Häussler, Phys. Lett. **222,** 65 (1992).
[16] A. G. Jljinskii, S. J. Slyusarenko, W. Hinz, and W. Hoyer, Metallophysica **14,** 35 (1992).
[17] Y. Waseda, The structure of non-crystalline materials, McGraw-Hill Inc., New York 1980.